

# A combined experimental and computational study of the substituent effect on photodynamic efficacy of amphiphilic Zn(II)phthalocyanines

Anzhela Galstyan,<sup>\*a,b</sup> Kristina Riehemann,<sup>b</sup> Michael Schäfers<sup>a,c,d</sup>  
and Andreas Faust<sup>a,c,d</sup>

<sup>a</sup>European Institute for Molecular Imaging, Waldeyerstr.15, 48149 Münster (Germany),  
[anzhela.galstyan@wwu.de](mailto:anzhela.galstyan@wwu.de)

<sup>b</sup>Physikalisches Institut and CeNTech, Westfälische Wilhelms-Universität Münster, Heisenbergstrasse  
11, 48149 Münster (Germany).

<sup>c</sup> Department of Nuclear Medicine, University Hospital Münster, Albert-Schweitzer-Campus 1, 48149  
Münster

<sup>d</sup> DFG EXC 1003 'Cells in Motion' Cluster of Excellence, University of Münster, Germany

## Supporting Information

### Table of Contents

1. Photophysical Data	S2
1.1 Absorption spectra	S2
1.2 Excitation and emission spectra	S3
1.3 Time resolved luminescence decays	S4
1.4 Determination of singlet molecular oxygen quantum yields	S7
2. Partition coefficient	S8
3. Theoretical studies	S8
4. <i>In vitro</i> studies	S10
5. Analytical data	S11

# 1. Photophysical Data

## 1.1. Absorption spectra

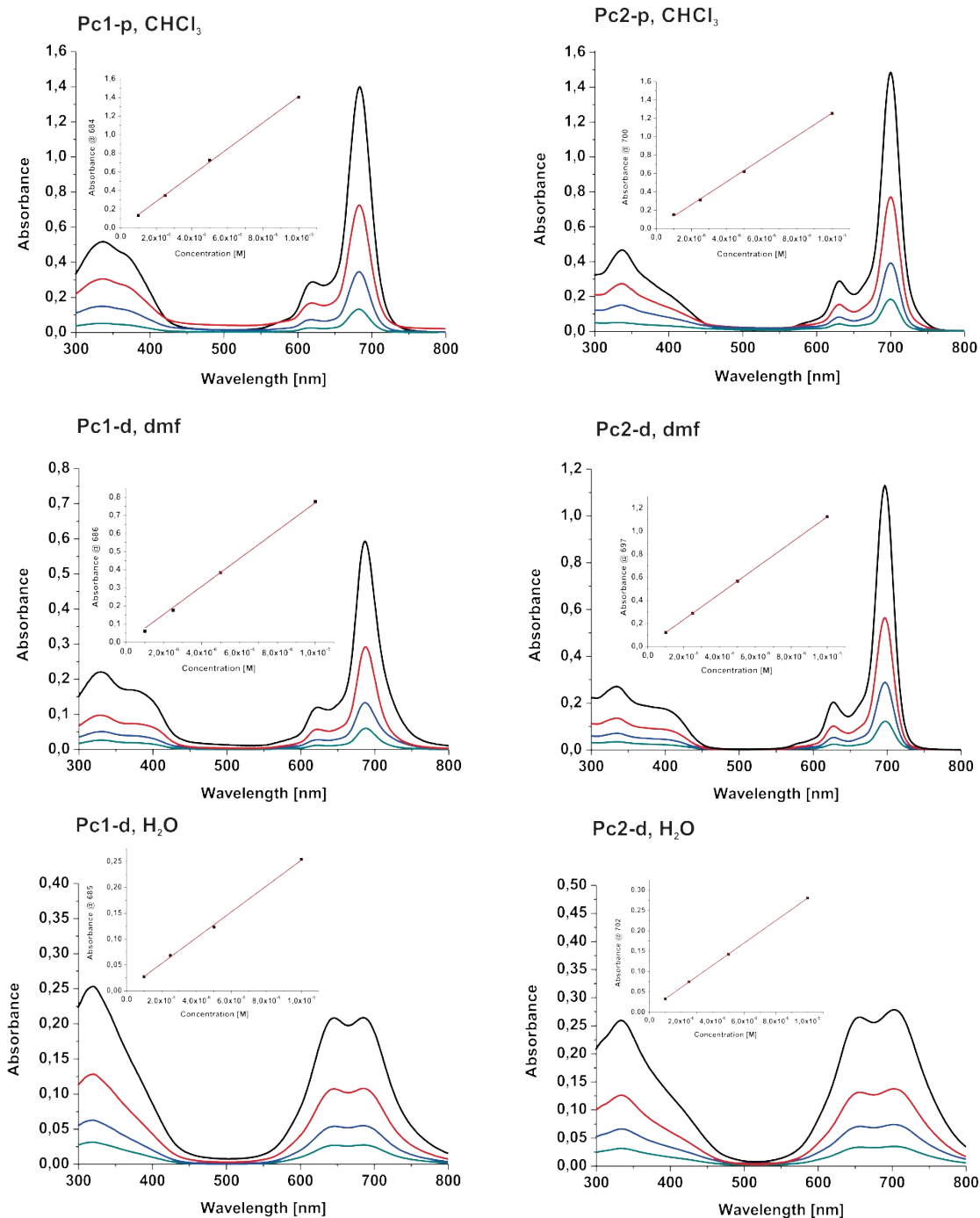


**Figure S1.** UV-Visible spectra of **Pc1-p**, **Pc2-p**, **Pc1-d** and **Pc2-d** in different solvents (CHCl<sub>3</sub>, DMF and H<sub>2</sub>O) at different concentrations (1 to 10 μM). The inset of each spectrum plots the Q-band absorbance vs the concentration of the Zn(II)phthalocyanine and the line represents the best-fitted straight line.

## 1.2. Excitation and emission spectra

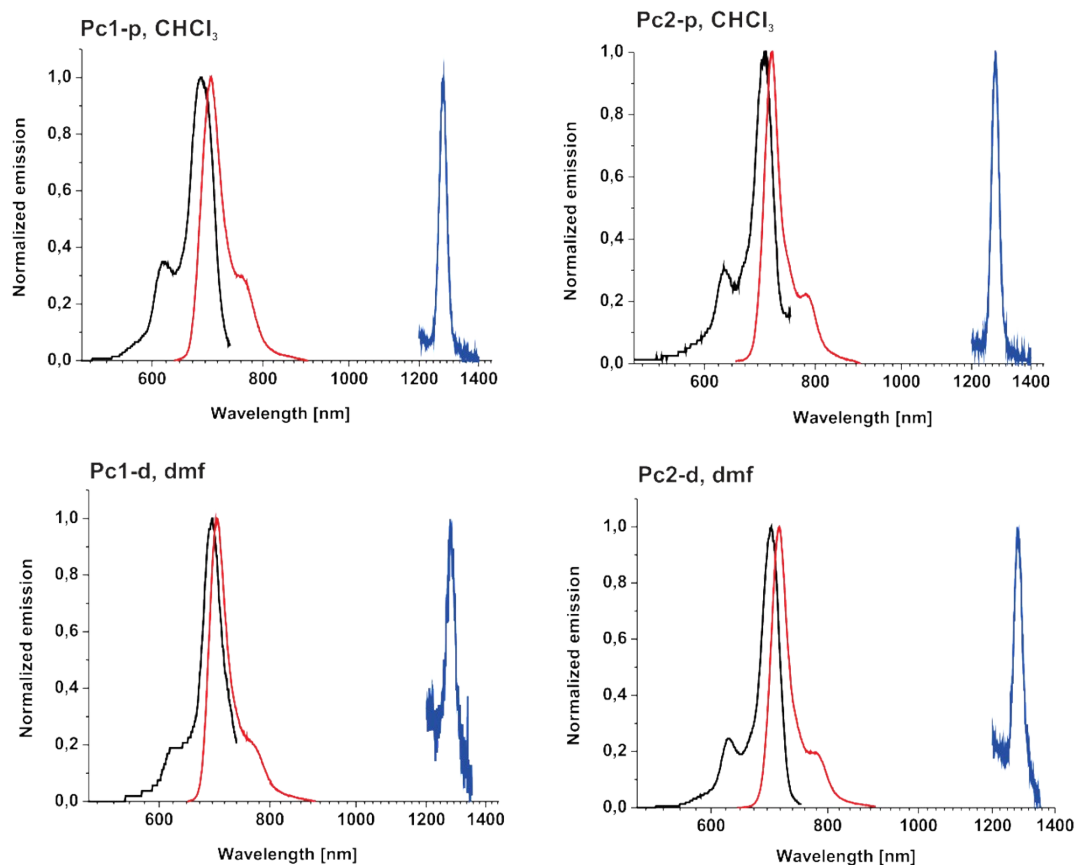
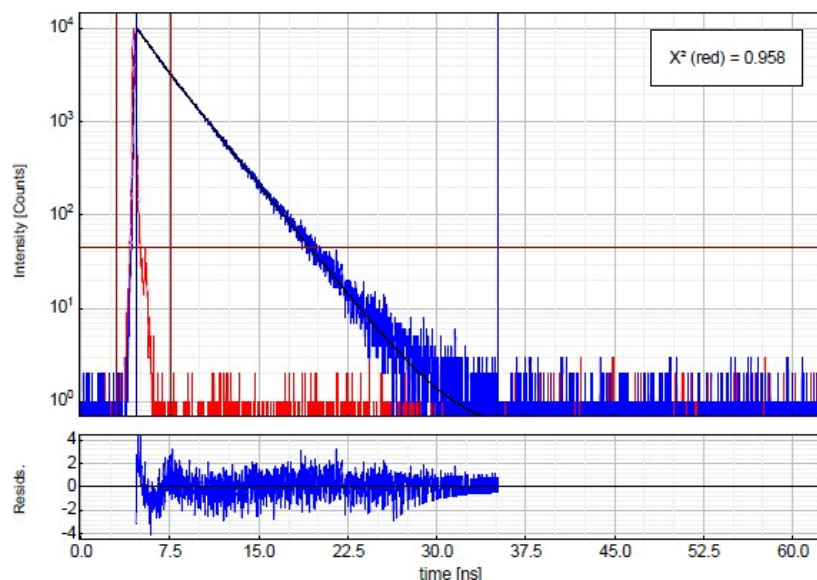


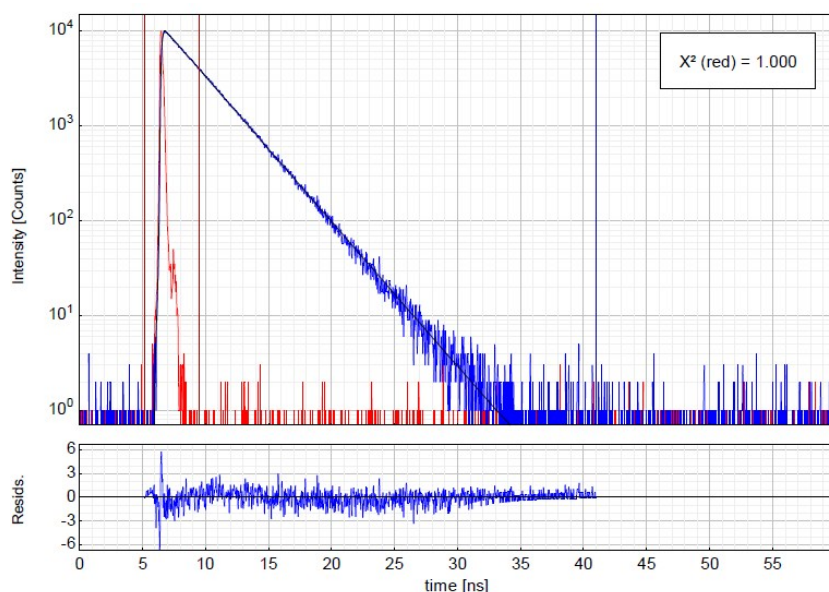
**Figure S2.** Excitation, fluorescence and singlet oxygen emission spectra of **Pc1-p** ( $\lambda_{\text{exc}}=610\text{nm}$ ,  $\lambda_{\text{em}}=760\text{nm}$ ) and **Pc2-p** ( $\lambda_{\text{exc}}=625\text{nm}$ ,  $\lambda_{\text{em}}=784\text{nm}$ ) in  $\text{CHCl}_3$  and **Pc1-d** ( $\lambda_{\text{exc}}=610\text{nm}$ ,  $\lambda_{\text{em}}=760\text{nm}$ ) and **Pc2-d** ( $\lambda_{\text{exc}}=625\text{nm}$ ,  $\lambda_{\text{em}}=785\text{nm}$ ) in DMF.

### 1.3. Time resolved luminescence decays



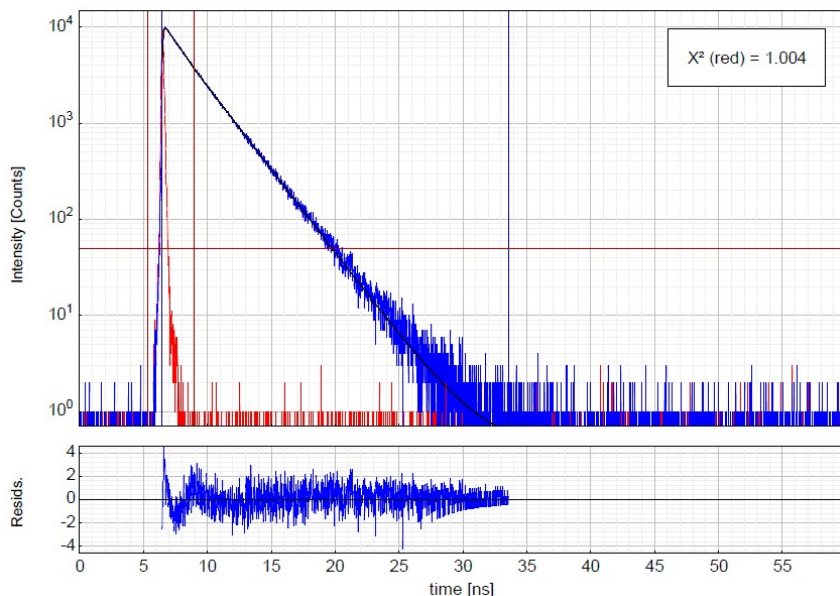
Parameter	Value	Conf. Lower	Conf. Upper	Conf. Estimation
$A_1$ [Cnts]	11470.9	-59.9	+59.9	Fitting
$\tau_1$ [ns]	2.75108	-0.00987	+0.00987	Fitting
Bkgr. Dec [Cnts]	0.477	-0.431	+0.431	Fitting
Bkgr. IRF [Cnts]	45.49	-2.10	+2.10	Fitting
Shift IRF [ns]	-0.1187	-0.0134	+0.0134	Fitting

**Figure S3.** Time-resolved luminescence decay of **ZnPc1-p** in  $\text{CHCl}_3$  including the instrument response function and the residuals ( $\lambda_{\text{exc}}=635$  nm) and fitting parameters including pre-exponential factors and confidence limits.



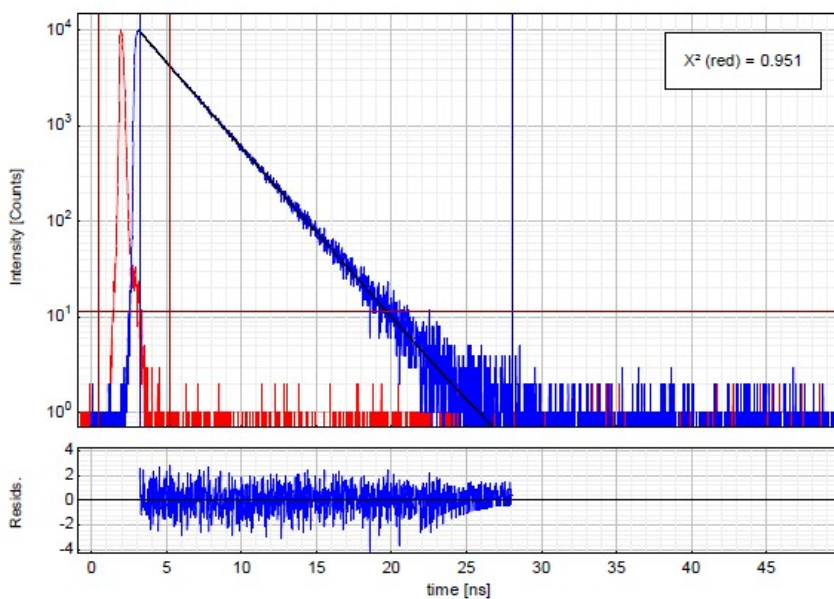
Parameter	Value	Conf. Lower	Conf. Upper	Conf. Estimation
$A_1$ [Cnts]	11435.2	-60.3	+60.3	Fitting
$\tau_1$ [ns]	2.8378	-0.0106	+0.0106	Fitting
Bkgr. Dec [Cnts]	0.0357	-0.381	+0.381	Fitting
Bkgr. IRF [Cnts]	0.496	-0.662	+0.662	Fitting
Shift IRF [ns]	0.01966	-0.00265	+0.00265	Fitting

**Figure S4.** Time-resolved luminescence decay of **ZnPc2-p** in  $\text{CHCl}_3$  including the instrument response function and the residuals ( $\lambda_{\text{exc}}=635$  nm) and fitting parameters including pre-exponential factors and confidence limits.



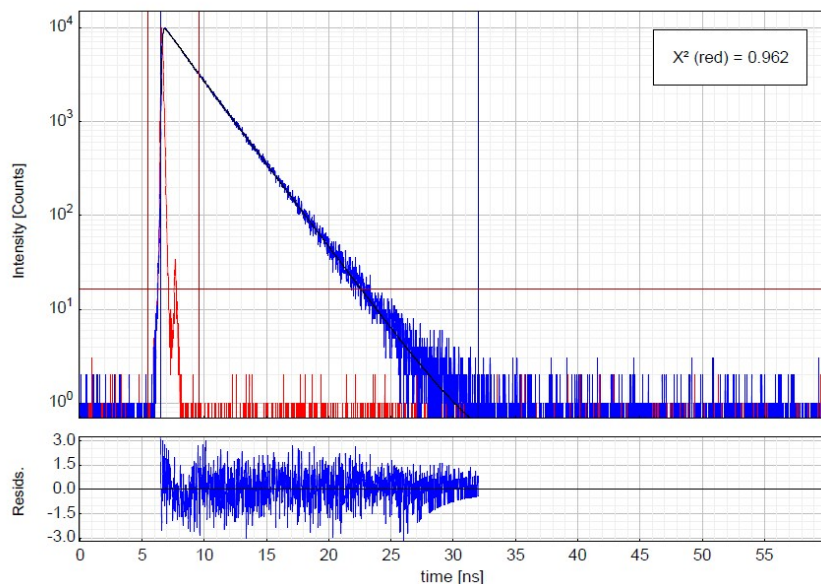
Parameter	Value	Conf. Lower	Conf. Upper	Conf. Estimation
A <sub>1</sub> [Cnts]	11342.5	-58.4	+58.4	Fitting
τ <sub>1</sub> [ns]	2.50436	-0.00919	+0.00919	Fitting
Bkgr. Dec [Cnts]	0.415	-0.459	+0.459	Fitting
Bkgr. IRF [Cnts]	49.09	-2.36	+2.36	Fitting
Shift IRF [ns]	-0.02066	-0.00300	+0.00300	Fitting

**Figure S5.** Time-resolved luminescence decay of **ZnPc1-d** in DMF including the instrument response function and the residuals ( $\lambda_{\text{exc}}=635$  nm) and fitting parameters including pre-exponential factors and confidence limits.



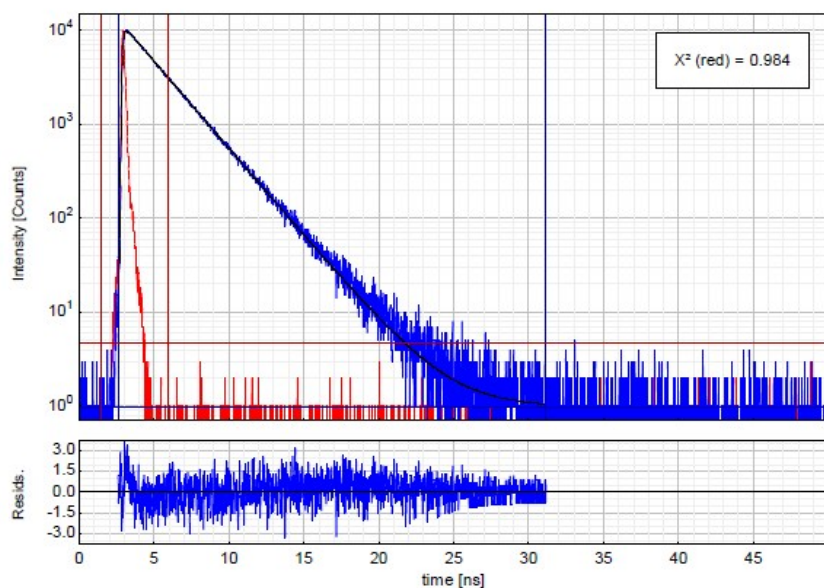
Parameter	Value	Conf. Lower	Conf. Upper	Conf. Estimation
A <sub>1</sub> [Cnts]	16067.1	-80.6	+80.6	Fitting
τ <sub>1</sub> [ns]	2.44662	-0.00687	+0.00687	Fitting
Bkgr. Dec [Cnts]	0.087	-0.479	+0.479	Fitting
Bkgr. IRF [Cnts]	11.44	-2.15	+2.15	Fitting
Shift IRF [ns]	-0.9254	-0.0120	+0.0120	Fitting

**Figure S6.** Time-resolved luminescence decay of **ZnPc2-d** in DMF including the instrument response function and the residuals ( $\lambda_{\text{exc}}=635$  nm) and fitting parameters including pre-exponential factors and confidence limits.



Parameter	Value	Conf. Lower	Conf. Upper	Conf. Estimation
A <sub>1</sub> [Cnts]	11208.7	-53.9	+53.9	Fitting
τ <sub>1</sub> [ns]	2.46851	-0.00846	+0.00846	Fitting
Bkgr. Dec [Cnts]	0.230	-0.484	+0.484	Fitting
Bkgr. IRF [Cnts]	16.31	-1.95	+1.95	Fitting
Shift <sub>IRF</sub> [ns]	-0.05793	-0.00221	+0.00221	Fitting
A <sub>Scat</sub> [Cnts]	-4080	-1520	+1520	Fitting

**Figure S7.** Time-resolved luminescence decay of **ZnPc1-d** in H<sub>2</sub>O including the instrument response function and the residuals ( $\lambda_{\text{exc}}=635$  nm) and fitting parameters including pre-exponential factors and confidence limits.



Parameter	Value	Conf. Lower	Conf. Upper	Conf. Estimation
A <sub>1</sub> [Cnts]	11325.3	-59.1	+59.1	Fitting
τ <sub>1</sub> [ns]	2.34455	-0.00873	+0.00873	Fitting
Bkgr. Dec [Cnts]	0.985	-0.435	+0.435	Fitting
Bkgr. IRF [Cnts]	4.73	-1.64	+1.64	Fitting
Shift <sub>IRF</sub> [ns]	0.13918	-0.00219	+0.00219	Fitting
A <sub>Scat</sub> [Cnts]	25250	-2210	+2210	Fitting

**Figure S8.** Time-resolved luminescence decay of **ZnPc2-d** in H<sub>2</sub>O including the instrument response function and the residuals ( $\lambda_{\text{exc}}=635$  nm) and fitting parameters including pre-exponential factors and confidence limits.

#### 1.4. Determination of singlet molecular oxygen quantum yields

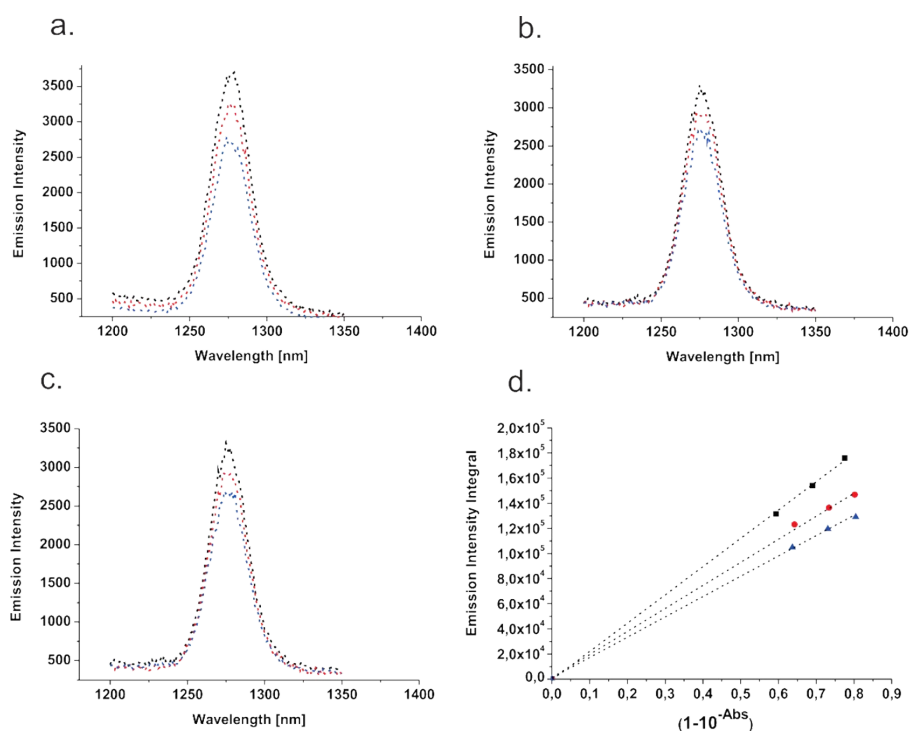


**Figure S9.** Phosphorescence spectrum of the photogenerated singlet oxygen for tetra-*t*-butylphthalocyaninato zinc(II) (a), **Pc1-p** (b) and **Pc2-p** (c) in CHCl<sub>3</sub> for three concentrations. Plots of the emission intensity against the fraction of absorbed light tetra-*t*-butylphthalocyaninato zinc(II) (black), **Pc1-p** (blue) and **Pc2-p** (red). The line represents the best-fitted straight line.

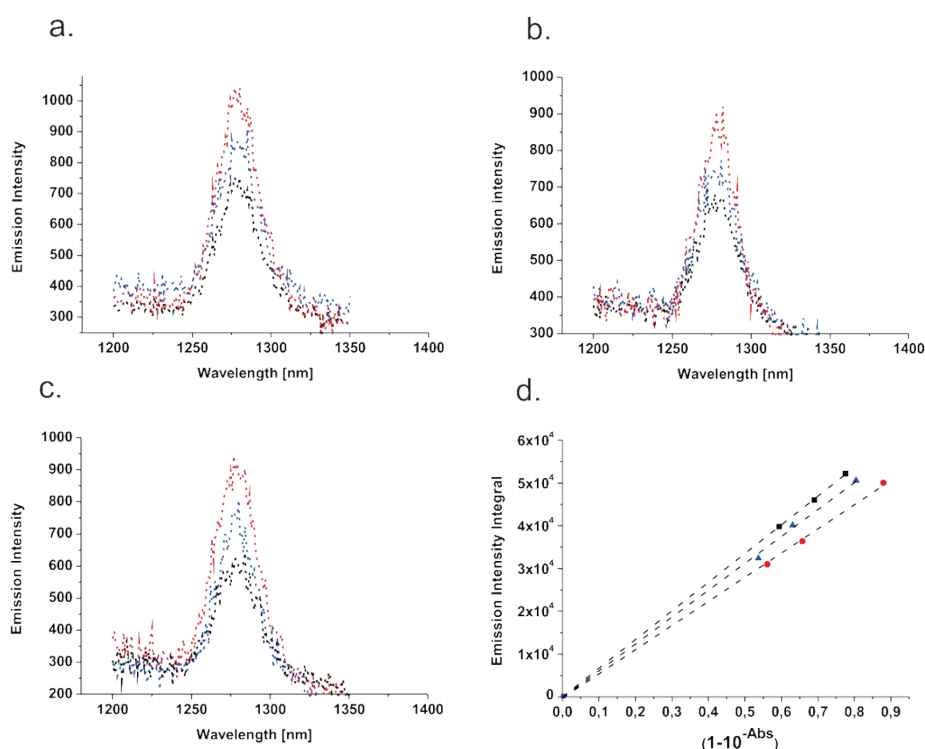


**Figure S10.** Phosphorescence spectrum of the photogenerated singlet oxygen for tetra-*t*-butylphthalocyaninato zinc(II) (a), **Pc1-d** (b) and **Pc2-d** (c) in DMF for three concentrations. Plots of the emission intensity against the fraction of absorbed light tetra-*t*-butylphthalocyaninato zinc(II) (black), **Pc1-d** (red) and **Pc2-d** (blue). The line represents the best-fitted straight line.

## 2. Partition coefficients

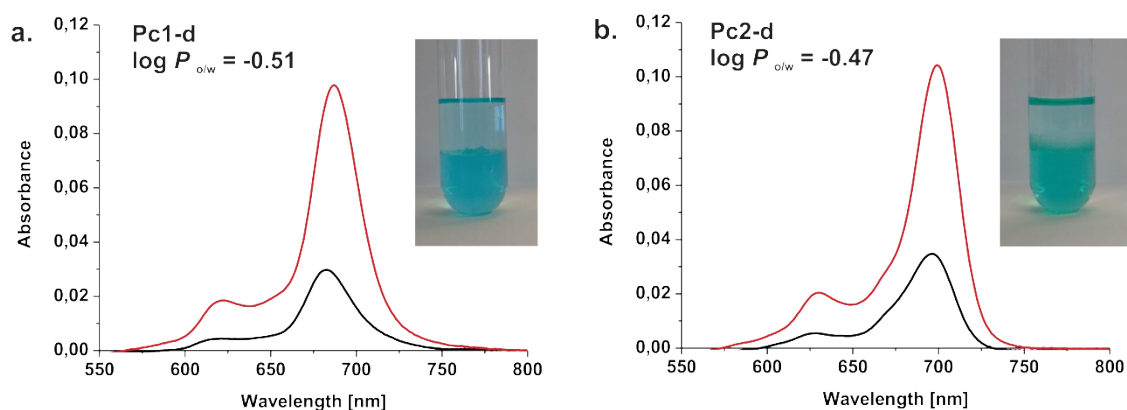


**Figure S11.** Absorption spectra of **Pc1-d** (a) and **Pc2-d** (b) from water phase – red line and 1-octanol phase – black line.

## 3. Binding to Human Serum Albumin

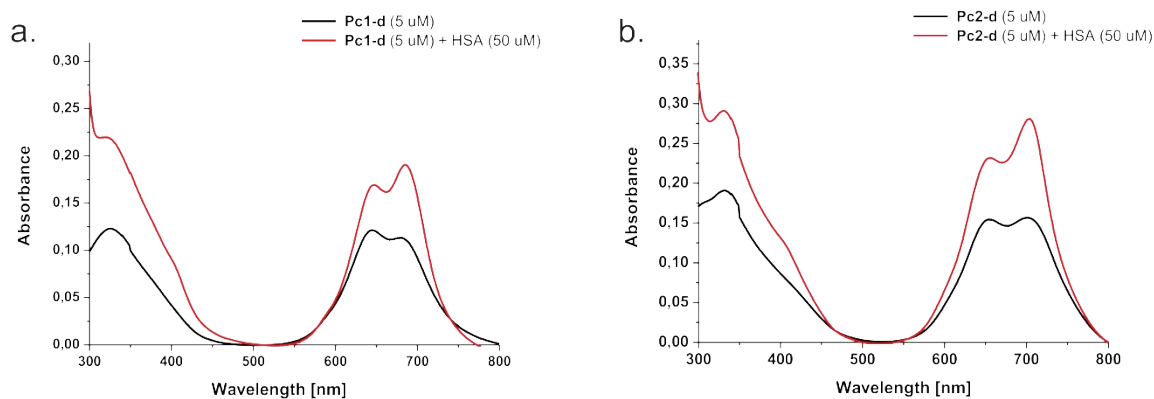


**Figure S12.** Absorption spectra of **Pc1-d** (a) and **Pc2-d** (b) in the absence (black line) and presence of HSA (red line).

## 4. Theoretical calculations

**Table S1.** List of selected molecular orbital energies and HOMO–LUMO energy gaps [eV] for the model system **Pc1-m** and **Pc2-m**.

Orbital	Pc1-m	Pc2-m
LUMO + 5	-0.7878	-1.0928
LUMO + 4	-0.8014	-1.2267
LUMO + 3	-0.8931	-1.2278
LUMO + 2	-1.1886	-1.2498
LUMO + 1	-2.8107	-2.7239

LUMO	-2.8216	-2.7451
HOMO	-4.9498	-4.7971
HOMO – 1	-6.3645	-5.8145
HOMO – 2	-6.4959	-5.8456
HOMO – 3	-6.5095	-6.1650
HOMO – 4	-6.5490	-6.4252
HOMO – 5	-6,8113	-6.7204
<hr/>		
HOMO-LUMO		
gap	2.1282	2.0520
<hr/>		

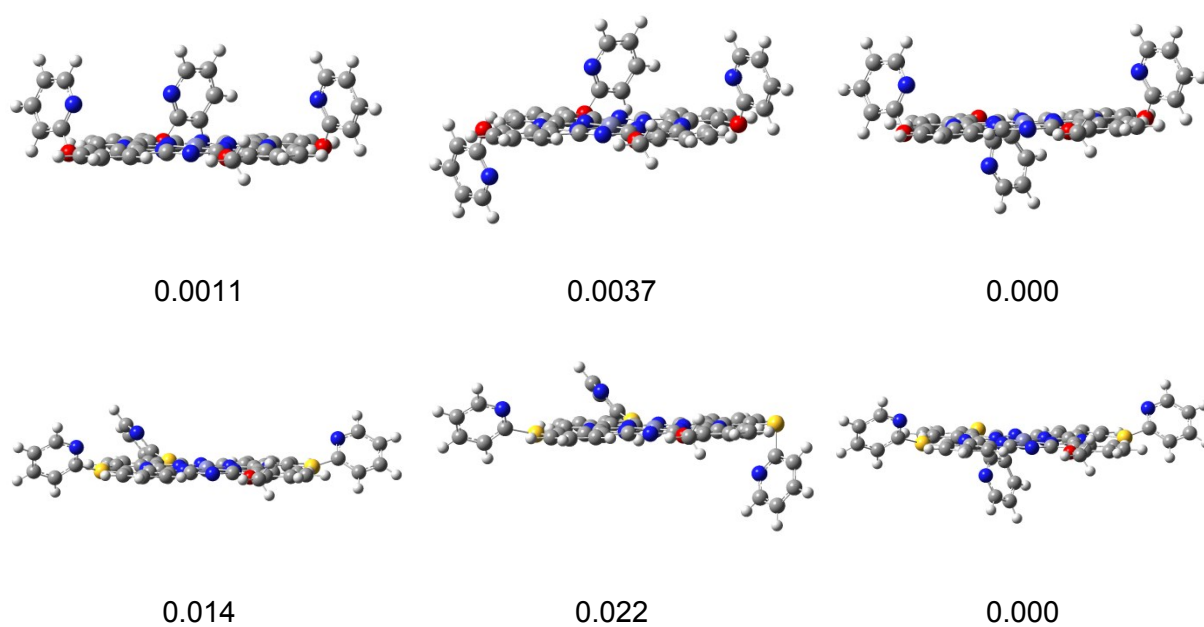


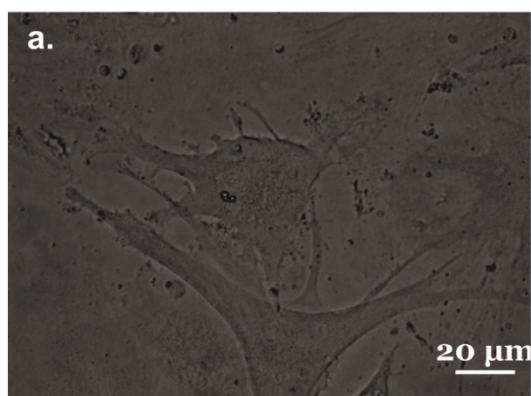
**Figure S13.** Optimized structures of different conformers of the model system **Pc1-m** and **Pc2-m** and the calculated relative energies ( $\text{kcal mol}^{-1}$ ) using B3LYP/6-311G(d,p).

## 5. *In vitro* studies

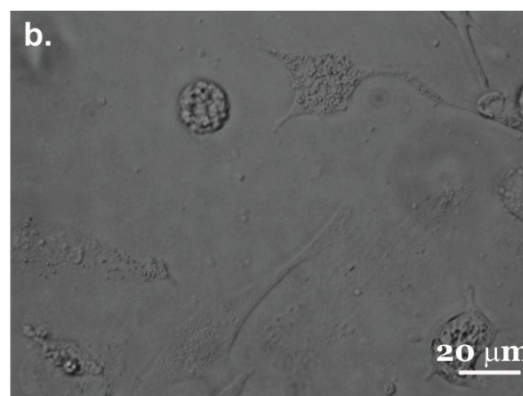
**Table S2.** Summary of the irradiation experiments.

Compound	Pos. Control	H <sub>2</sub> O Control	Neg. Control	10µg/ml	5µg/ml	1µg/ml	
<b>Pc1-d</b>	irradiated	0.00 (±0.16)	99.31 (±2.88 )	100.00 (±1.86)	17.28 (±3.60)	57.92 (±12.74)	93.97 (±4.06)
	dark	0.00 (±0.04)	106.15 (±9.11)	100.00 (±7.65)	97.92 (±8.63)	104.87 (±9.38)	108.98 (±14.78)
<b>Pc2-d</b>	irradiated	0.00 (±0.24)	104.56(±6.28)	100.00(±8.92)	2.43 (±1.95)	16.38 (±5.21)	77.98 (±7.39)
	dark	0.00 (±0.15)	111.61(±15.73)	100.00(±9.16)	88.86 (±7.89)	95.80(±11.20)	100.68(±3.90)

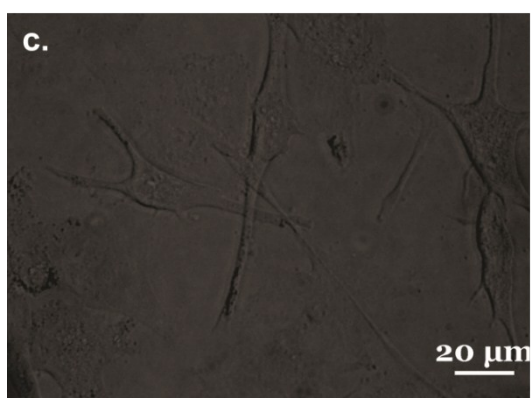
**Pc1-d** 0mg/ml 24h after irradiation



**Pc1-d** 10mg/ml 24h after irradiation



**Pc2-d** 0mg/ml 24h after irradiation



**Pc2-d** 10mg/ml 24h after irradiation

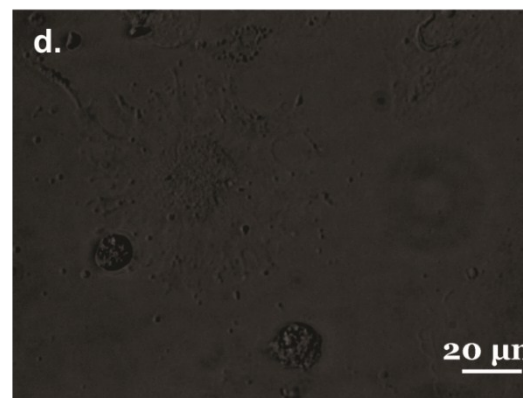


**Figure S14.** Morphological changes after PDT for COLO-818 cell line incubated with 10 mg/ml **Pc1-d** (b) and **Pc2-d** (d) 24h after irradiation. Negative controls for **Pc1-d** (a) and **Pc2-d** (c).

## 6. Analytical Data

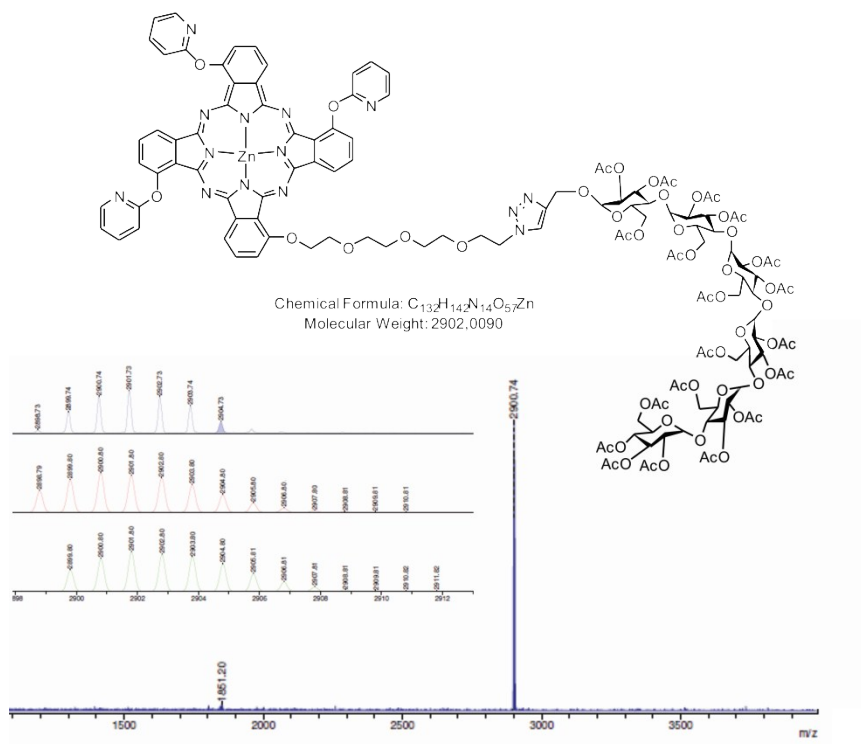


**Figure S15.** MALDI-MS spectra of **Pc1-p** measured in trans-2-[3-(4-tert-Butylphenyl)-2-methyl-2-propenylidene]malononitrile DCTB matrix ( $CHCl_3$ ). Insert: measured and calculated isotope pattern.

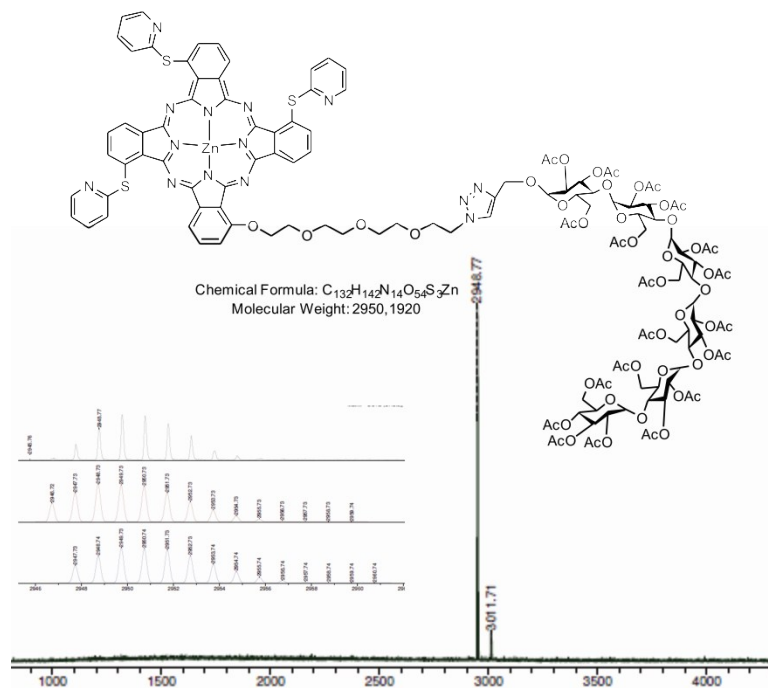


**Figure S16.** MALDI-MS spectra of **Pc2-p** measured in trans-2-[3-(4-tert-Butylphenyl)-2-methyl-2-propenylidene]malononitrile DCTB matrix ( $CHCl_3$ ). Insert: measured and calculated isotope pattern.

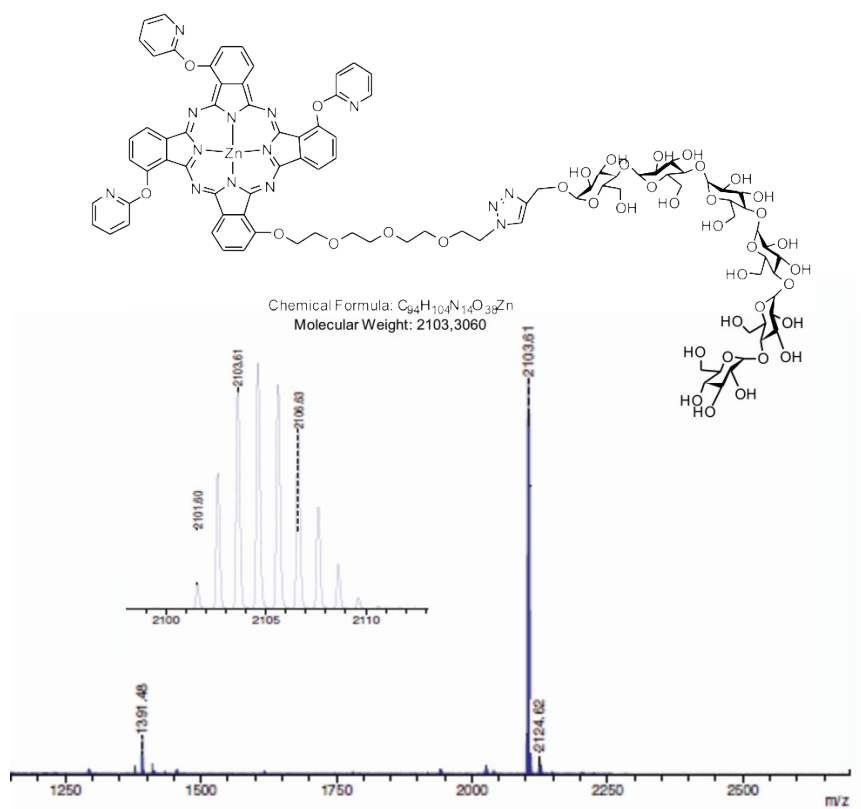


**Figure S17.** MALDI-MS spectra of **Pc1-d** measured in 2,5-Dihydroxybenzoic acid DHB matrix ( $H_2O/ACN$ ). Insert: measured isotope pattern.

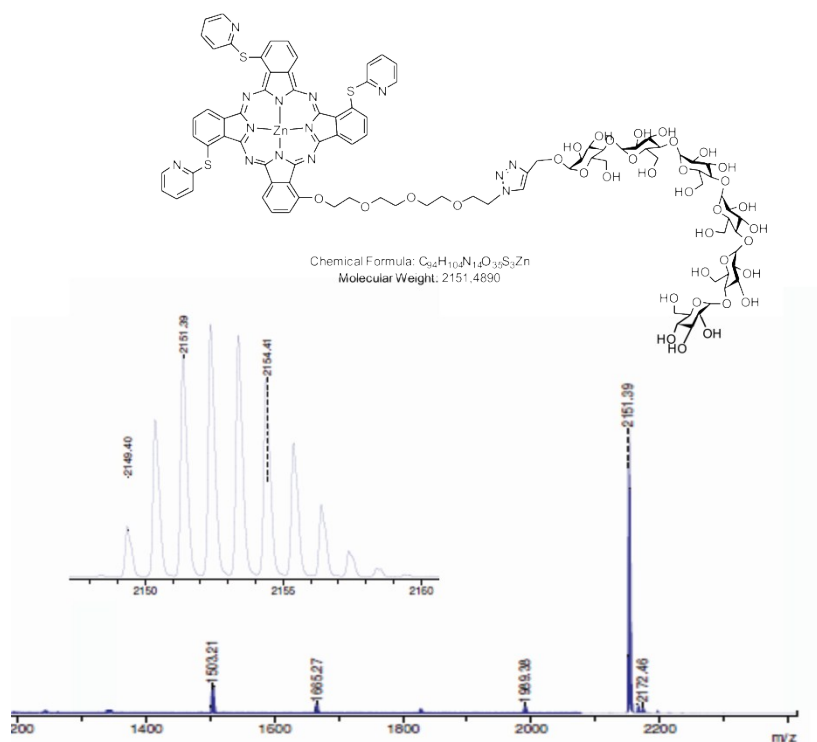


**Figure S18.** MALDI-MS spectra of **Pc2-d** measured in 2,5-Dihydroxybenzoic acid DHB matrix ( $H_2O/ACN$ ). Insert: measured isotope pattern.

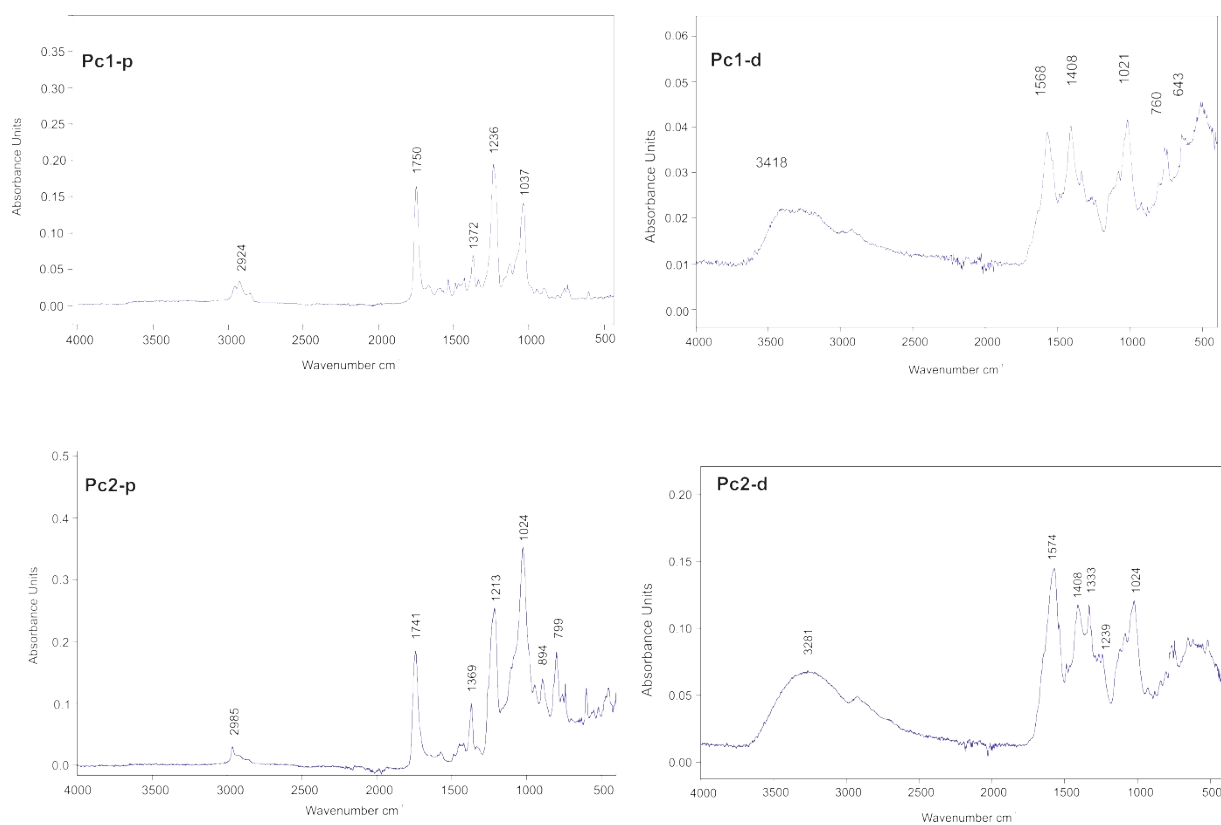


**Figure S19.** FT-IR spectra of **Pc1-p**, **Pc1-d**, **Pc2-p** and **Pc2-d**.

*1H NMR spectra show broad chemical shifts likely due to the self-aggregation at NMR concentration as well as presence of four positional isomers.*